Evaluation of Oat Kernel Size Uniformity

Douglas C. Doehlert,* Michael S. McMullen, Jean-Luc Jannink, Surangan Panigrahi, Huanzhong Gu, and Neil R. Riveland

ABSTRACT

Oat (*Avena sativa* L.) kernel size uniformity is important to the oat milling industry because oat-processing mills separate oats according to size to optimize dehulling efficiency. In this study, we compared two different approaches for analyzing oat kernel size uniformity, namely the sequential sieving of oat samples with a gradient of slotted sieve sizes and digital image analysis. Image analysis of size fractions provided evidence that sieving separated oat kernels according to their depth, whereas, digital image analysis measured kernel length and width, and derived a measure of the area of the oat kernel image. Samples identified by sieving with superior uniformity were those with greater proportions of large kernels. Histograms of oat kernel sizes derived from digital image analysis suggested oat kernel sizes were (within a genotype and location) composed of bimodal populations. A new statistical analysis allowed for the derivation of means and variances of each of these subpopulations, the numerical balance between the two subpopulations, and the extent of bimodality. Oat samples with lower levels of bimodality tended to be of higher test weight and groat percentage and thus, of better milling quality. Both methods appear satisfactory for evaluating oat kernel size uniformity, although the sequential sieving method is likely to be more useful to breeding programs because of its relative technical ease and simplicity.

Oat kernel size uniformity is important to the oat milling industry because the processing of oats for human food generally involves size separation of kernels into different streams before dehulling (Hachmann, 1947; Peek and Poehlman, 1949; Deane and Commers, 1986; Salisbury and Wichser, 1971). This is because smaller oat kernels require faster impact dehuller rotor speeds to obtain the same dehulling efficiency as larger kernels (Bruckner, 1953; Ganssmann and Vorwerck, 1995). Dehulling oats with excessive mechanical stress results in excessive groat breakage, whereas insufficient mechanical stress results in lower dehulling efficiency (Doehlert et al., 1999; Doehlert and McMullen, 2001). Thus, sizing oats allows for fine-adjustment of the optimal rotor speed for each size fraction to maximize dehulling efficiency and milling yield.

Oat kernel size is, however, inherently nonuniform because of the multifloret habit of the oat spikelet. Oat spikelets may contain one, two, three, or more kernels. The outermost of these, called the primary kernel, is the largest, and mass decreases with higher orders of kernels. The study of Doehlert et al. (2002) indicated that primary kernels of triple kernel spikelets were the largest and were significantly larger than primary kernels of double kernel spikelets. Secondary kernels from triple kernel spikelets were not significantly different in size from primary kernels of single kernel spikelets, and these were larger than secondary kernels from double kernel spikelets. Tertiary kernels were the smallest kernel type studied. However the double kernel spikelet is by far the most abundant spikelet type in most oat genotypes (Takeda and Frey, 1980; Doehlert et al., 2002).

Early studies evaluating oat size uniformity emphasized size differences between primary and secondary kernels (Zade, 1915; Mader, 1927; Milatz, 1933). Later studies evaluated mass distributions of oat fractions separated by sequential sieving with slotted sieves (Sword, 1949; Hubner, 1951; Bruckner et al., 1956; Ganssmann, 1964; Doehlert et al., 2002). More recently, digital image analysis has been applied to size analysis of oat kernels (Symons and Fulcher, 1988; Pietrzak and Fulcher, 1995; Doehlert et al., 1999).

It is important to define dimensions of oat kernel size here because many different characteristics have been used to express size. The nomenclature used here is consistent with that introduced by de Villers (1935). He suggested kernel length to be the distance from the base to the tip of the lemma, the width being perpendicular to the crease and lemma venation when the kernel is lying with its crease down. The depth of the oat kernel was defined as being the distance from the dorsal to the ventral side of the oat kernel, taking the palea as the dorsal and the lemma as the ventral side. Different types of analyses measure different combinations of these dimensions. Kernel mass may be the best evaluation of kernel size, which is essentially a three-dimensional measurement (multiplied by kernel density). Digital image analysis, at best, measures only two dimensions. These are typically length and width, although kernel image area can also be derived from those data. Although it has not been characterized experimentally, it seems reasonable to presume that sequential sieving would separate kernels by their smallest dimension, being their depth. Thousand-kernel weight is a measure of the mean kernel mass of an oat sample, but distributions of individual kernel masses have not been measured in oats to the knowledge of the authors. Such measurements can be made in wheat with an automated single kernel analyzer (Martin et al., 1993). Such an instrument has been used to evaluate groat mass distributions (Doehlert, unpublished data), but oat hulls and trichomes tend to interfere with the pneumatic systems of this type of instrument, making the application impractical.

D.C. Doehlert, USDA-ARS Wheat Quality Laboratory, Harris Hall, M.S. McMullen, Department of Plant Sciences, S. Panigrahi and H. Gu, Department of Agricultural Engineering, North Dakota State University, Fargo ND 58105; J.L Jannink, Agronomy Department, Iowa State University, Ames IA 50011-1010; N.R. Riveland, Williston Research Extension Center, 14120 Highway 2, Williston, ND 58801. The mention of firm names or trade products does not imply that they are endorsed or recommended by the U.S. Department of Agriculture over other firms or similar products not mentioned. Received 15 May 2003. *Corresponding author (douglas.doehlert@ndsu.nodak.edu).

Published in Crop Sci. 44:1178–1186 (2004).

677 S. Segoe Rd., Madison, WI 53711 USA

In this study we attempted to evaluate oat kernel size uniformity by both sequential sieving and digital image analysis, and to relate these with mean kernel mass whenever possible. Our objectives were to determine genotypic and environmental effects on oat kernel size distributions as measured by these two methods and to relate these characteristics with other quality characteristics in oat grain.

MATERIALS AND METHODS

Plant Material

Ten oat cultivars (AC Assiniboia, Belle, CDC Boyer, Derby, Hytest, Jerry, AC Medallion, Otana, Triple Crown, and Youngs) were grown at five locations (Carrington, Edgeley, Fargo, Minot, and Williston) in North Dakota in, 1999, 2000, and 2001. A seeding rate of 2.47×10^6 kernels ha^{-1} was used for all experiments. Herbicide treatments consisted of preemergence application of 3.93 kg ha^{-1} propchlor (2-chloro-*N*-isopropylacetanilide) and post-emergence application at the 3-leaf stage with a tank mix of 0.14 kg ha^{-1} thifensulfuron {methyl 3 [[[[(4-methoxy-6-methyl-1,3,5-triazin-2yl)amino]carbonyl]amino]sulfonyl]-2-thiophenecarboxylate}, 0.07 kg ha^{-1} tribenuron {methyl 2-[[[[N-(methoxy-6-methyl-1,3,5-triazin-2yl) methylamino] carbonyl] amino] sulfonyl] benzoate}, and 0.14 kg ha^{-1} clopyralid (3,6-dichloro-2-pyridinecarboxylic acid, monoethanolamine salt). Experimental units consisted of four rows spaced 0.3 m apart and 2.4 m long. The two center rows were harvested with a two-row binder and threshed with a plot thresher. The harvested grain was cleaned using a Clipper (Bluffton, IN) Model 400 Office Tester and Cleaner fitted with a 4.75×, 19-mm oblong hole sieve and with aspiration adjusted so that kernels containing a groat were not removed. The sieve allowed all grain to pass through.

Analyses

Grain yield was determined from the mass of grain harvested from the center two rows of the test plots, after cleaning. Test weight was determined by weighing a fixed volume of grain from a test weight filling hopper (Seedburo Equipment Company, Chicago, IL). Volumes of grain from size fractionation were not sufficient to fill the filling hopper required for test weight measurements, so bulk densities were determined on size fractions by dividing mass of a grain sample by its volume, as measured in a graduated cylinder. Crown rust (causal agent *Puccinia coronata* Cda. f. sp. *avenae* Eriks.) infection score was determined in the field at close to the peak infection time. Plots were scored from 0 to 5, where 0 indicated a plot free of crown rust and 5 indicated the heaviest possible infection. Groat percentage on field plot samples were determined with a compressed air dehuller (Codema, Eden Prairie, MN) correcting for hulled grain remaining after dehulling described as the final groat percentage in Doehlert and McMullen (2001). Groat percentages of size fractions were determined by hand dehulling, as described in Doehlert et al. (1999). Mean kernel mass was determined by counting the number of kernels in a 10-g sample. Kernels were counted with an automated seed counter (Seedburo Equipment Company, Chicago, IL).

Grain was fractionated into size fractions with slotted sieves and a sizer-shaker (Seedburo Company, Chicago, IL). Grain samples of 150 g were sieved sequentially on slotted 3.18-, 2.58-, 2.38-, and 1.98-mm sieves. All slots were, 19.05 mm long. Grains held back by these sieves were labeled as oversized, large, medium, and small, respectively. Kernels that passed through the 1.98-mm sieve were labeled as undersized. Sieve sizes used for separations were designed to mimic commercial systems as described by Deane and Commers (1986). The uniformity product (Doehlert et al., 2002) was calculated as the product of the percent large kernels, the percent medium kernels, and the percent small kernels.

Digital image analysis was used to measure the length, width, and image area of individual oat kernels in samples. Ten-gram samples of oat kernels were placed on a backlit glass platform within a predefined field of view. A scale (in mm) was also attached to the platform. An analog camera (using photographic film) was mounted at a fixed height of one meter from the platform. Oat kernels were manually positioned on the platform ensuring seeds were not touching each other and a photograph taken. The developed 10.2- by 15.2-cm photographic prints were digitized as 8-bit gray images with a resolution of 236 pixels per cm with scanner and were saved in a tiff format.

A separate image processing program was developed to determine the required measurements (lengths and widths) of each seed automatically from an image. The program was developed in macro environment of a commercial image processing software Aphelion (Amerinex Applied Imaging, Amherst, MA). The image was initially processed with a 3x3 low pass filter to reduce the noise. A separate program (not available in the Aphelion software) was incorporated within the Aphelion environment. This program is a histogram-based automatic background segmentation algorithm (Otsu, 1979). Using this program, a threshold is automatically selected to remove the background of this image. Thus, the segmented image only contained the objects (oat kernels). Subsequent image analysis programs–functions were used to extract each kernel as a region and determine its major and minor axes. The determined major axis represented the length and the minor axis represented the width of each kernel. It is to be noted that the determined parameters were in pixels. Thus, the program had the capability to obtain the scale conversion factor (from pixel to cm or mm). Extensive validation experiments were performed to assure that analyses generated accurate measurements of oat kernel length, width, and image area. Manual measurements of metal rectangles, pieces of toothpicks, and oat kernels made with slide calipers and with manual operation of the imaging software were compared the automated analysis from images. The average difference between the manual and the automated measurements was 1.6 and 7.6% of the manual measurement for length and width, respectively. Considering a scale conversion factor of 1 pixel = 0.12 mm, the average difference (between manual and automated measurements) for length and width measurements were 0.14 and 0.17 mm, respectively. Means and variances were calculated from collected individual data for each sample. Typically samples contained 250 to 400 kernels. Images also were collected of size fractions derived from the sequential sieving procedure, and analyzed as above.

Histograms showing size distributions of combined size fractions required a normalization of frequencies according to their occurrence in original samples. Proportions of size fraction, collected as mass proportions, were converted to proportion according to kernel number on the basis of mean kernel masses of the size fractions. Frequencies of kernel sizes in sequential sieving fractions, expressed as percentages of mass, were multiplied by the kernel number proportion of each fraction. The summation of these fraction proportions matched well with frequencies of sizes in the original sample (data not shown).

Test for Bimodality

Histograms of oat kernel size observations suggested that these data were not normally distributed, and we sought a statistical test for bimodality. The following test was performed on all original unfractionated samples and compares the likelihood that the data fit a single normal distribution with the likelihood that every data point belongs to either of two normally distributed subpopulations, each with its own mean and variance. The single normal distribution model (Model u) assumes the data have mean μ and variance σ^2: $Y \sim N(\mu, \sigma^2)$. The likelihood function for this model is

$$L_u = \prod_{i=1}^{n} \frac{1}{\sqrt{2\pi\sigma^2}} \exp\left(-\frac{(y_i - \mu)^2}{2\sigma^2}\right) \quad [1]$$

where the data set contains n observations y_i ($i = 1 \ldots n$). Obtaining estimates of μ and σ^2 that maximize L_u amounts to calculating the usual $\hat{\mu} = \frac{1}{n}\sum y_i$ and $\hat{\sigma}^2 = \frac{1}{n-1}\sum (y_i - \hat{\mu})^2$. The mixture of two normal distributions model (Model b) assumes that each data point belongs to one of two subpopulations $P_1 \sim N(\mu_1, \sigma_1^2)$ or $P_2 \sim N(\mu_2, \sigma_2^2)$ with probabilities of belonging to P_1 and P_2 of p and $1 - p$, respectively. The likelihood for this model is

$$L_b = \prod_{i=1}^{n} \left[p \frac{1}{\sqrt{2\pi\sigma_1^2}} \exp\left(-\frac{(y_i - \mu_1)^2}{2\sigma_1^2}\right) + (1 - p) \frac{1}{\sqrt{2\pi\sigma_2^2}} \exp\left(-\frac{(y_i - \mu_2)^2}{2\sigma_2^2}\right) \right] = \prod_{i=1}^{n} [pf(y_i|P_1) + (1 - p) f(y_i|P_2)] \quad [2]$$

where $f(y_i|P_j)$ is the normal density function conditional on y_i belonging to population j. An expectation-maximization procedure was used to obtain estimates of $\hat{p}$, $\hat{\mu}_1$, $\hat{\sigma}_1^2$, $\hat{\mu}_2$, and $\hat{\sigma}_2^2$ that maximize L_b, as follows. Initial values are chosen for $\hat{p}$, $\hat{\mu}_1$, $\hat{\sigma}_1^2$, $\hat{\mu}_2$, and $\hat{\sigma}_2^2$. In practice, we took $\hat{p} = 0.5$, $\hat{\mu}_1 = \hat{\mu} - \hat{\sigma}$, $\hat{\sigma}_1^2 = \hat{\sigma}^2$, $\hat{\mu}_1 = \hat{\mu} + \hat{\sigma}$, and $\hat{\sigma}_2^2 = \hat{\sigma}^2$, though we verified that different initial values did not affect the final estimates obtained. The procedure then alternates the following two steps. In step one, the probability p_i that each observation i belongs to P_1 is calculated as

$$p_i = \frac{\hat{p} f(y_i|P_1)}{f(y_i)} \quad [3]$$

where $f(y_i) = pf(y_i|P_1) + (1 - p) f(y_i|P_2)$. In step two, the estimates for $\hat{p}$, $\hat{\mu}_1$, $\hat{\sigma}_1^2$, $\hat{\mu}_2$, and $\hat{\sigma}_2^2$ are updated as follows:

$$\hat{p} = \frac{1}{n} \sum_{i=1}^{n} p_i \quad [4]$$

$$\hat{\mu}_1 = \frac{1}{n\hat{p}} \sum_{i=1}^{n} p_i y_i \quad [5]$$

$$\hat{\sigma}_1^2 = \frac{1}{n\hat{p} - 1} \sum_{i=1}^{n} p_i (y_i - \hat{\mu}_1)^2 \quad [6]$$

Updating $\hat{\mu}_2$, and $\hat{\sigma}_2^2$ is done as for $\hat{\mu}_1$ and $\hat{\sigma}_1^2$, except that $\hat{p}$ and p_i are replaced by $1 - \hat{p}$ and $1 - p_i$ in Eq. [5] and [6]. Note that, to be maximum likelihood estimators in the strict sense, Equation [6] should not have –1 in its denominator, and likewise for the variance estimator in Model u above. The –1 factor corrects for the well-known downward bias in maximum likelihood estimators and otherwise has no impact on the validity of the test. To retain biological relevance, we constrained updates in step two such that $0.1 \leq \hat{p} \leq 0.9$ and $\min(\hat{\sigma}_1^2, \hat{\sigma}_2^2)/\hat{\sigma}^2 \geq 0.02$. These steps were iterated until stable estimates are obtained. In practice, we iterated until L_b changed by less than 10^{-8} between iterations. A likelihood ratio can be calculated from L_u and L_b as follows:

$$T = 2 \ln\left(\frac{L_b}{L_u}\right) \quad [7]$$

The distribution of (T) in (7) when observations are in fact normally distributed is currently the object of debate (McLachlan and Peel, 2000). For the specific problem at hand, we obtained the null distribution of T by repeatedly simulating normally distributed data sets and applying the test to them. Five thousand simulations were performed, producing a distribution of T that in its tail resembled a χ^2 with four degrees of freedom, with a threshold for Type I error rate $\alpha = 0.05$ of 9.0.

Note that, strictly speaking, the test outlined above is not a test for bimodality per se but of the presence of a mixture of normal distributions. In the present context in which there are biological mechanisms causing kernel measures to be bimodal, de facto the test assesses bimodality. That said, support for Model b entails the following interpretation. The oat kernels harvested represent a mixture of two types, small and large. Each type has its own mean size and variance about that mean as given by the parameters $\hat{\mu}_1$, $\hat{\sigma}_1^2$, $\hat{\mu}_2$, and $\hat{\sigma}_2^2$. Among all kernels, $\hat{p}$ represents the fraction that belongs to the small type. Thus, the biological mechanism that leads to the genesis of small type kernels may be considered more active in genotypes with high $\hat{p}$. The T statistic provides a measure of the extent to which small and large types are clearly differentiated in a given data set or genotype. Genotypes where $\hat{\mu}_1$ is close to $\hat{\mu}_2$ (as scaled by the overall standard deviation in kernel size) will have a low T and, conversely, when $\hat{\mu}_1$ and $\hat{\mu}_2$, are strongly divergent, a high T will arise. In what follows, we refer to $\hat{p}$ as "Prob1." and to T as the *bimodality coefficient*.

Experimental Design and Statistical Analyses

Field plots were arranged in a random complete block design with three replicates. Analysis of variance was applied to data where genotypes were considered fixed and environments were considered random. Analyses of variance were calculated with the Statistix computer package (Analytical Software, Tallahassee, FL), where the environment × replicate mean square was used as an error term to test the environmental effect. The genotype × environment interaction mean square was used to test the genotypic effect, and the genotype × environment interaction was tested with the residual mean square. Mean separation was evaluated by the least significant difference, which was also calculated by the Statistix software program using the previously described error terms. For correlations across genotypes, correlations were first calculated for characteristics within each environment. A Chi square test was performed to verify that correlation coefficients were not significantly heterogeneous across environments (Steel et al., 1997). When heterogeneity was not observed, correlation coefficients were pooled over environments according to Steel et al. (1997). For correlations across environments, correlations were first calculated individually for each genotype, the pooled over genotypes by the procedure just described.

RESULTS

General Characteristics of Genotypes and Environments

Before analyzing kernel size uniformity, general agronomic and grain quality characteristics were analyzed

Table 1. Genotypic means of grain yield and quality characteristics from 10 oat cultivars grown in 15 environments (five locations, 3 yr) in North Dakota.

Genotype	Yield	Test weight	Crown rust	Groat percentage	Kernel mass
	Mg ha^{-1}	kg m^{-3}	Score	%	mg
AC Assiniboia	4.59	481	0.0	72.8	34.8
Belle	4.01	479	0.5	71.5	28.8
CDC Boyer	3.79	456	1.8	70.2	33.5
Derby	3.41	432	2.6	62.7	28.7
Hytest	3.08	517	2.6	72.6	31.1
Jerry	3.73	494	2.5	69.8	29.1
AC Medallion	4.09	471	0.1	69.1	31.4
Otana	3.12	418	3.4	59.5	24.7
Triple Crown	4.19	461	0.7	68.4	31.6
Youngs	4.16	457	1.5	67.4	34.0
LSD (0.05)	0.04	21	0.6	3.0	1.4

to evaluate how kernel size uniformity relates to these more general characteristics. Genotypic means of grain yield (Table 1) and correlation analysis (not shown) indicated that grain yields were negatively correlated with crown rust infection ($r = -0.630$, $P < 0.01$). In contrast, test weight was only weakly correlated with crown rust infection ($r = -0.222$, $P < 0.05$). Although the lowest test weight values were obtained from cultivars relatively susceptible to crown rust (Derby and Otana), the highest test weights were also obtained from cultivars relatively susceptible to crown rust (Hytest and Jerry). Cultivars with superior crown rust resistance (AC Assiniboia, Belle, AC Medallion) also exhibited consistently high test weights (Table 1). Across genotypes, groat percentage correlated well with test weight ($r = 0.723$, $P < 0.01$). Different cultivars exhibited very specific trends in kernel mass, where AC Assiniboia, CDC Boyer, and Youngs had the largest kernels whereas Derby and Otana had the smallest kernels. Genotype × environment interactions were significant for all these characteristics, and were largely attributed to differing crown rust resistance among cultivars and differing crown rust infection pressure in the different environments. The magnitude of the interactions (not shown) was less than 5% of the total variation and was not considered to affect conclusions concerning the main effects.

Environmental means of yield indicated significant variation (Table 2), attributed largely to weather conditions and incidence of crown rust, which is also heavily influenced by weather conditions. The low yield from Minot 1999 was attributed to hail damage. The highest test weights were obtained from the Minot and Williston locations, which had significantly lower incidences of crown rust. As observed with genotypic means, across environments groat percentages significantly correlated with test weight ($r = 0.439$, $P < 0.01$). Mean kernel masses were generally larger at Minot and Williston, which had lower incidences of crown rust. Across environments mean kernel mass was significantly correlated negatively with crown rust infection ($r = -0.523$, $P < 0.01$) and positively correlated with test weight ($r = 0.693$, $P < 0.01$).

Size Analysis

Results of sequential sieving indicated that this procedure could be used to generate crude distributions of size frequencies (Table 3). All genotypes exhibited frequencies of oversized kernels of less than 1%, which is consistent with the elite nature of these cultivars. Considerable variation was observed in proportions of large kernels among genotypes (Table 3). Correlation analysis indicated that mean kernel weight was positively correlated with the percentage of large kernels ($r = 0.524$, $P < 0.01$) and with percentage of medium kernels ($r = 0.687$, $P < 0.01$). Similarly, proportions of small and undersized kernels were negatively correlated with mean kernel weight ($r = -0.621$ and –0.858, respectively, $P < 0.01$), where cultivars with small mean kernel mass (Belle and Otana) also had the largest proportion of undersized kernels.

The uniformity index was designed to evaluate for the equal distribution of grain among the three size fractions that would be used for oat milling. More equal distributions among these fractions would allow for more efficient milling from three streams, since all streams would be of about the same mass. The highest uniformity indexes were associated with genotypes that have larger proportions of large kernels ($r = 0.898$, $P < 0.01$), whereas uniformity indexes were negatively associated with proportions of small kernels ($r = -0.941$, $P < 0.01$) and undersized kernels ($r = -0.831$, $P < 0.01$).

Table 2. Environmental means of grain yield and quality from 10 oat cultivars grown in 15 environments (five locations, 3 yr) in North Dakota.

Environment	Yield	Test weight	Crown rust	Groat percentage	Kernel mass
	Mg ha^{-1}	kg m^{-3}	Score	%	mg
Carrington '99	5.05	470	1.6	69.4	31.9
Carrington '00	3.37	454	2.0	64.2	30.3
Carrington '01	4.62	434	3.2	64.7	28.2
Edgeley '99	2.30	417	1.9	65.7	27.1
Edgeley '00	3.84	434	2.1	68.1	29.4
Edgeley '01	4.98	471	2.7	70.1	31.6
Fargo '99	3.26	458	1.9	61.5	28.1
Fargo '00	3.91	436	3.0	69.8	26.9
Fargo '01	3.76	449	0.7	62.3	27.1
Minot '99	1.82	489	1.5	66.0	30.6
Minot '00	4.62	512	1.2	68.9	34.5
Minot '01	5.59	468	1.7	72.8	31.6
Williston '99	3.33	489	0.0	72.5	33.1
Williston '00	3.80	468	0.0	72.6	36.8
Williston '01	4.23	507	0.0	77.5	34.3
LSD (0.05)	0.32	22	0.3	3.2	1.2

Table 3. Genotypic means of mass proportions of oat grain samples in different size fractions as generated by sequential sieving with slotted sieves. Oversized kernels were held back by a 3.18-mm slotted sieve, large kernels by a 2.58-mm slot, medium kernels by a 2.38-mm slot, small kernels by a 1.98-mm slot. Undersized kernels passed through the 1.98-mm slot. All slots were 19.05 mm in length.

Genotype	Over sized	Large	Medium	Small	Under sized	Uniformity product
AC Assiniboia	0.2	33.9	31.1	31.0	4.5	26 711
Belle	0.0	4.4	19.7	61.3	14.6	4 741
CDC Boyer	0.3	35.2	26.4	33.0	5.1	25 941
Derby	0.3	12.3	27.6	49.5	10.6	14 907
Hytest	0.2	11.5	32.2	48.5	7.7	16 079
Jerry	0.3	6.7	24.8	59.4	8.9	9 480
AC Medallion	0.2	26.5	25.8	40.1	8.5	24 319
Otana	0.2	9.7	15.6	58.6	16.2	8 056
Triple Crown	0.8	12.9	30.7	49.4	6.8	18 299
Youngs	0.6	15.6	33.9	43.1	6.5	20 150
LSD (0.05)	0.2	5.7	5.5	6.6	2.2	4 419

Table 4. Environmental means of mass proportion distributions of oat kernels after size fractionation by sequential sieving with slotted sieves. Oversized kernels were held back by a 3.18-mm slotted sieve, large kernels by a 2.58-mm slot, medium kernels by a 2.38-mm slot, small kernels by a 1.98-mm slot. Undersized kernels passed through the 1.98-mm slot. All slots were 19.05 mm long.

Environment	Over sized	Large	Medium	Small	Under sized	Uniformity product
Carrington '99	0.4	26.7	33.3	34.2	4.8	20 427
Carrington '00	0.6	20.1	28.7	43.0	7.3	19 575
Carrington '01	0.4	22.6	23.9	43.8	9.1	18 514
Edgeley '99	0.4	13.2	23.3	50.4	11.7	14 932
Edgeley '00	0.4	12.9	25.6	50.5	10.4	15 472
Edgeley '01	0.3	18.6	30.6	43.6	6.9	20 306
Fargo '99	0.1	6.2	16.4	62.7	15.3	6 993
Fargo '00	0.2	9.1	19.7	56.9	14.6	10 716
Fargo '01	0.2	13.5	16.9	60.8	14.7	13 598
Minot '99	0.3	18.3	27.5	45.3	8.3	17 593
Minot '00	0.4	16.8	30.1	45.5	7.1	17 831
Minot '01	0.2	20.9	33.2	40.2	5.5	17 486
Williston '99	0.3	14.2	29.7	48.6	7.1	17 473
Williston '00	0.1	16.0	27.8	49.3	6.7	20 010
Williston '01	0.3	23.9	35.0	35.9	4.9	22 100
LSD (0.05)	0.2	3.5	2.6	4.2	1.3	2 121

Much less variation was found in environmental means of size distributions (Table 4). Most differences in the uniformity product could be attributed to higher undersized proportions, and less variation was observed in the large size proportions.

Genotypic and environmental means of kernel length, width, and area derived from digital image analysis (data not shown) were largely consistent with the mean kernel mass data (Tables 1 and 2), where genotypes with more massive kernels had kernels with larger lengths, widths and areas. Mean length, width, and areas were also calculated for all size fractions generated from sequential sieving. These are of relatively low interest, in that they show only the obvious size differences that would be expected between different size fractions and are shown only as grand means of all genotypes from all locations (Table 5). One important observation to be drawn from the width data is that the mean kernel width was larger than the sieve that they passed through. That is to say that the mean width of medium kernels is 3.08 mm (Table 5), yet these kernels have already passed through a slot of 2.58 mm. This would suggest that sieving did not separate kernels according to their width, but by their depth, which was smaller than the width. Similarly, it would appear that small kernels, with a width of 2.85 mm, could not have passed through a 2.38-mm sieve unless their depth was less than 2.38 mm. Analysis of bulk densities and groat percentages of the different size fractions indicate that both increased with decreasing kernel size fraction (Table 5).

Histograms of length, width, and area distributions of size fractions presented as stacked bar graphs provide much more information as to kernel size uniformity and the relation of digital image analysis data to sequential sieving (Fig. 1 and 2). The summation of these fractions, evident from the height of each bar, appears indicative of bimodal populations at least with respect to area and length, as if oat size distributions were composed of two subpopulations. Distributions of width were less distinctively bimodal. Size fractions derived from sieving were not restricted to single subpopulations. Even undersized kernels were found in distributions associated with both subpopulations. This is consistent with the observation that the standard deviation of image area within a size fraction was only slightly smaller than the standard deviation for the original sample (Table 5). Ranges for the different size fractions span a large proportion of the range of the original sample (Fig. 1 and 2). Many size fractions also had bimodal appearances, especially with respect to area measurements. The distributions of widths among the different size fractions indicate that most kernels in those size fractions were larger than the slots that they had passed through to become in that size fraction. Thus, it appeared unlikely that sieving can separate by width, but by a smaller dimension, namely depth. Therefore, these histograms provide a three-dimensional picture of size distributions, where length and width are measured by the digital image analysis information and sieving provides an estimation of kernel depth.

The hypothesis that oat kernel image area size distributions are composed of bimodal populations was tested with a statistical analysis that fitted image area distributions as mixtures of two populations with distinctive means and variances. The results of this analysis for area distributions (Table 6) are largely consistent with this hypothesis. Bimodality coefficients (Table 6) were consistently highly significant, suggesting that the oat size populations were composed of (at least) two distinct subpopulations. Values of Prob1 indicate the probability that a particular kernel would be in the first or smaller subpopulation. Most genotypes had Prob1 values close to 0.5. However, two genotypes had mean Prob1 values less than 0.4 (Otana and Derby). These genotypes with smaller Prob1 values were also more distinctly bimodal, as determined by the magnitude of the bimodality coefficients. Those genotypes with lower bimodality coefficients, and had size distributions of less distinctive bimodal appearance, were cultivars that either had larger kernels (AC Assiniboia and Youngs) or had higher fre-

Table 5. Grand means of physical characteristics of original oat samples and their size fractions. Large kernels were held back by 2.58-mm slots, medium by 2.38-mm slots and small kernels were held back by 1.98-mm slots. All slots were 19.05 mm long.

	Mass distribution	Kernel mass	Kernel length	Kernel width	Kernel area	Kernel area SD	Bulk density	Groat percentage
	%	mg kernel^{-1}	mm		mm^2		g L^{-1}	
Original	–	30.7	10.3	2.90	22.4	5.4	526	73.8
Large	16.9	39.3	11.4	3.17	26.8	4.3	486	70.4
Medium	26.8	36.3	10.8	3.08	24.9	4.1	532	74.0
Small	47.4	28.7	9.9	2.85	21.1	4.6	551	76.1
LSD (0.05)	1.1	0.3	0.1	0.01	0.2	0.04	8	0.8

quencies of triple kernel spikelets (Belle) as determined in Doehlert et al. (2002).

DISCUSSION

Both sequential sieving and digital image analysis provided useful evaluations of oat kernel size uniformity. It appeared that they measured quite different dimensions of oat size, with sieving separating according to kernel depth, and digital image measuring by width and length. Digital image analysis had the advantage of superior resolution, in that individual kernels are measured. It allowed for the measurement of many individual kernels, which can be used in rigorous statistical analyses. It has the disadvantages of requiring costly equipment and/or significant technical expertise. Whereas, sequential sieving requires relatively inexpensive equipment, its resolution limited by the sizes of sieves available. There are only two or three more commercially available sieves not used in this study, which would be within the size range of oat kernels. Sieving is also less technically challenging and less time consuming than digital image analysis, so that operations limited by time and/or funds might find it a more practical procedure for

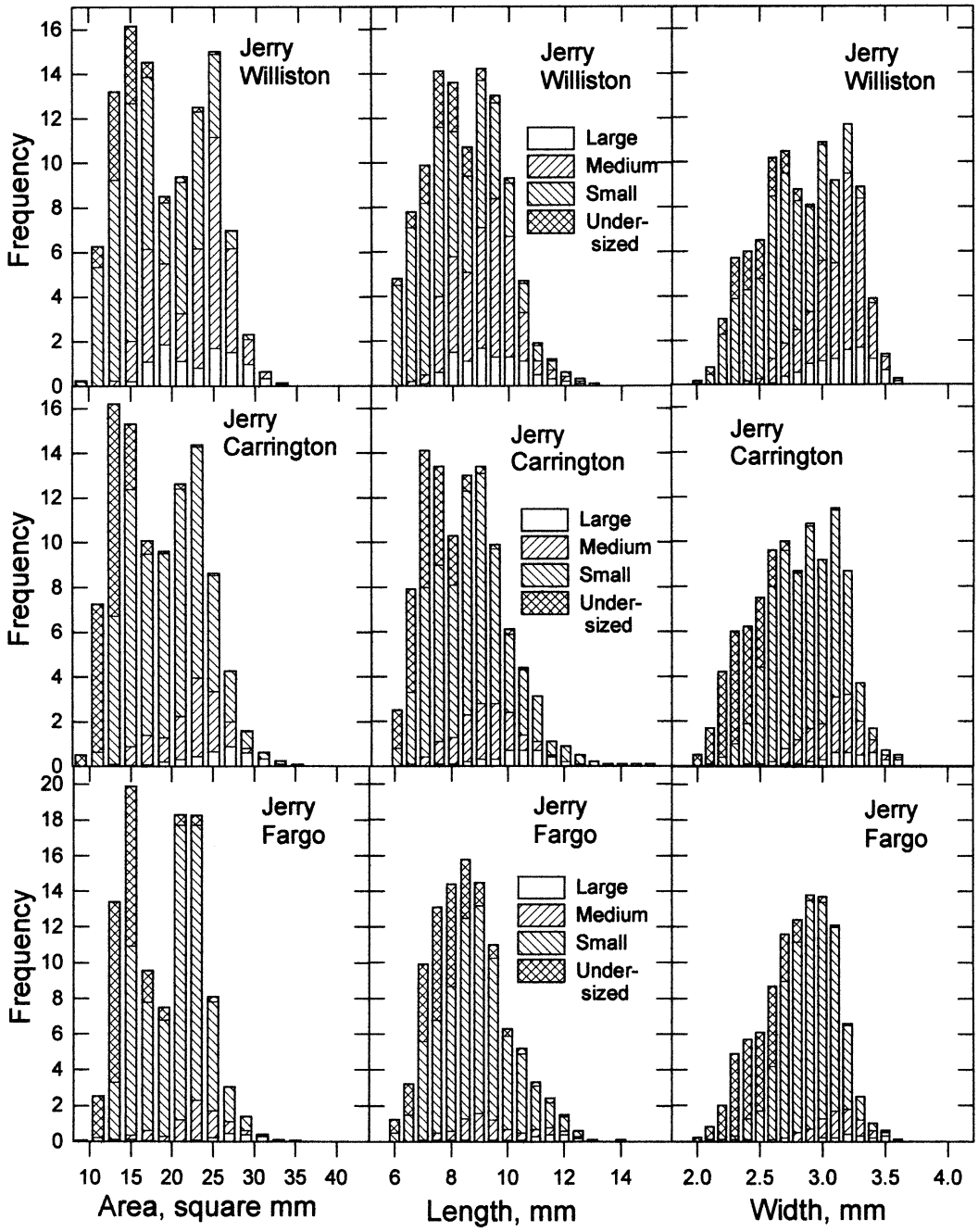

Fig. 1. Histograms showing distributions of oat kernel length, width and image areas from sample of Jerry oat grown at Fargo, Carrington, and Williston, ND, in the year 2000. Also shown within each bar is the frequency of each size fraction (large, medium, small and undersized) as separated by sequential sieving.

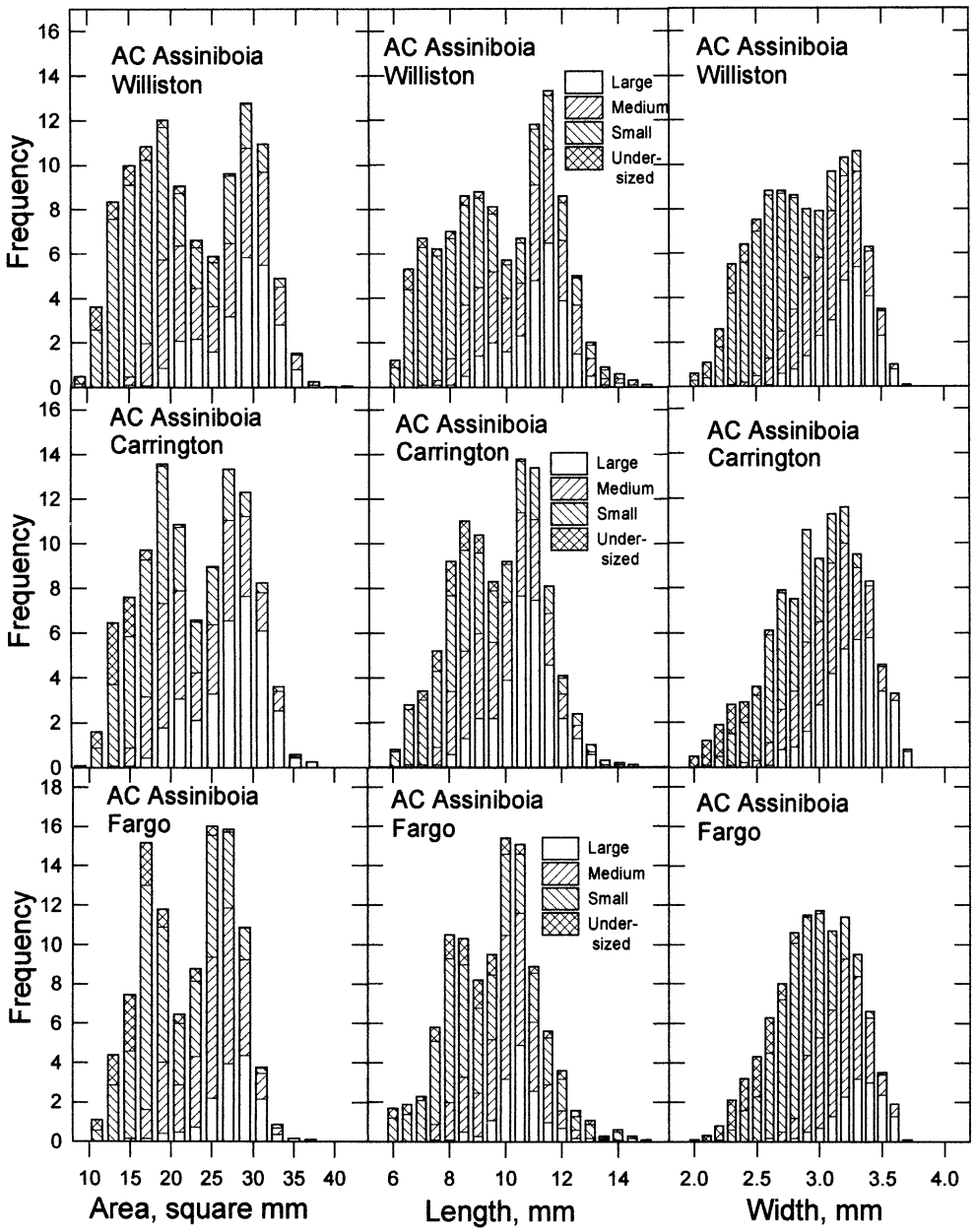

Fig. 2. Histograms showing distributions of oat kernel length, width and image areas from sample of AC Assiniboia oat grown at Fargo, Carrington, and Williston, ND, in the year 2000. Also shown within each bar is the frequency of each size fraction (large, medium, small and undersized) as separated by sequential sieving.

evaluating grain size uniformity. Many grain analysis labs possess sieve sizers already, whereas digital image analysis systems are less frequently found, and can be very costly to establish.

Samples with higher uniformity indexes may be more easily processed because those samples had kernels more evenly distributed across a range of expected kernel sizes. These samples also had higher variances of size parameters as determined by image analysis. The cultivars with higher uniformity products were also the ones with more large kernels (Table 3). Milling of cultivars with higher frequencies of smaller kernels could overwhelm the small or stub milling stream, leading to poorer operational efficiency.

Consistent with the hypothesis that digital image analysis and sequential sieving analyze different dimensions of the oat kernel is the differences in the shape of the distributions derived from these methods. Digital image analysis for area and length frequently appeared to be bimodal or multimodal (Fig. 1 and 2). Distributions from sequential sieving appeared to be unimodal (Tables 3 and 4). Although the resolution presented in this study allows for only five size classes, we have separated samples into as many eight fractions, and these have always appeared unimodal in shape (data not shown). Kernel width, as analyzed by digital image analysis, usually were unimodal in shape (Fig. 1 and 2), in spite of a high level of resolution allowed by digital image analysis. Distributions of oat kernel depth may be similar to width in this respect.

Table 6. Genotypic means of the parameters from the test for bimodality on oat kernels image area (square mm) data. The analysis tests data sets derived from digital image analysis to determine whether a model consisting of two distinct subpopulations described the sample better than a normal distribution. The analysis estimated means and variances for each subpopulation (group 1 and group 2) and a probability that a kernel was in group 1 (Prob1). Higher bimodality coefficients indicated a greater degree of bimodality. The empirically determined threshold value ($P < 0.05$) for the bimodality coefficient was 9.0.

Genotype	Area mean	Area variance	Mean Group 1	Variance Group 1	Mean Group 2	Variance Group 2	Prob 1	Bimodality coefficient
AC Assiniboia	24.1	37.1	19.5	14.2	29.6	8.3	0.536	49
Belle	20.9	21.6	17.2	9.8	24.6	6.4	0.515	38
CDC Boyer	23.2	32.8	17.6	6.7	27.7	9.8	0.443	76
Derby	23.0	30.9	16.7	5.1	26.8	9.7	0.380	104
Hytest	21.1	24.0	16.8	7.0	25.3	5.9	0.488	64
Jerry	20.5	23.6	15.7	5.1	24.2	7.0	0.439	92
AC Medallion	22.3	31.7	17.0	6.9	26.8	8.7	0.453	78
Otana	22.9	28.0	17.5	6.0	26.7	8.7	0.411	72
Triple Crown	21.3	24.0	15.7	4.8	24.3	8.8	0.356	90
Youngs	24.8	40.0	19.5	15.6	29.8	10.8	0.500	45
LSD(0.05)	0.4	2.0	0.5	2.4	0.3	1.3	0.042	15

We presume the basis of the bimodal populations depicted by the digital image analyses to lie with the size differences among the different order of kernels within the individual oat spikelet. Because most oat spikelets contain two kernels, the larger mode in the bimodal population may represent primary kernels from these double kernel spikelets, whereas the second mode may represent secondary kernels from these spikelets. Such distributions would be expected to be complicated by the presence of single and triple kernel spikelets that could add additional modes and increase ranges of sizes. An earlier study from this laboratory (Doehlert et al., 2002) analyzed spikelets from many of the same plots used in this study from the year 2000. This study indicated a high frequency of double kernel spikelets at the Fargo location, and a higher frequency of triple kernel spikelets at the Williston location. Figures 1 and 2 in this study show that samples taken from Williston showed a greater range (and standard deviation) than the samples analyzed from the Fargo location, but there is no evidence for additional modes in the Williston samples.

Introduction of bimodal analysis has facilitated the interpretation of data from digital image analysis. Because area and length measurements frequently do not fit normal distributions, traditional statistical analyses have failed to provide meaningful descriptions of the data. The bimodal analysis (Table 6) provides statistics that give an estimation of the extent of bimodality (bimodality coefficient) and gives an estimation of the balance in the numerical size of the two subpopulations (Prob1). The mean sizes of each of the two subpopulations (Mean Group1, Mean Group2) could be used to evaluate differences in sizes between primary and secondary kernels, as proposed by Milatz (1933).

Although we have had no direct test to indicate what size distributions are better for milling, we would speculate that higher Prob1 values would be desirable because that would indicate a more even distribution of kernel sizes. High values of the bimodality coefficient would indicate a highly bimodal population, which could separate easily and consistently into two subpopulations. However, correlation analysis indicated that in this study the bimodality coefficient was negatively correlated with test weight ($r = -0.45$, $P < 0.01$) and groat percentage ($r = -0.48$, $P < 0.01$). Thus, unless quality problems associated with extreme bimodality are alleviated, the highly bimodal distribution would act as a signal of poorer quality grain. Although samples of the best milling quality observed in this study with higher test weights and groat percentages had higher Prob1 values and lower bimodality coefficients, it is not known if those distributions offer any milling advantage directly associated with the distribution pattern.

It is difficult at this stage of study to conclude what size distributions are best for milling, primarily because no study of oat kernel size distributions in relation to milling yield has appeared in the literature. Also, optimal distribution for one mill might be quite different than that for another facility, because different operations will size fractionate into different numbers of streams. It is likely that most oat mills have the ability to efficiently mill almost any distribution pattern that is delivered to them, but as with any large scale industrial process, small increases in efficiency can result in large increases in profitability. Thus, a better understanding of oat kernel size distributions has significant potential return in processing efficiency.

REFERENCES

Bruckner, G. 1953. Der Einfluss der Korneigenschaften auf die Schalung des Hafers. Die Muhle und Mischfuttertechnik 90:434–436.

Bruckner, G., C. Nernst, M. Rohrlich, and E. Timm. 1956. Technologische und chemische Eigenschaften von Hafersorten. Jahrb. Versuch. Getreid. Berlin, 1954–1956:19–38.

Deane, D., and E. Commers. 1986. Oat cleaning and processing. p. 371–412. *In* F.H. Webster (ed.) Oats: Chemistry and technology. American Association of Cereal Chemists, St. Paul, MN.

de Villers, P.J.R.J. 1935. A genetic study of the inheritance of various characters in certain Avena hybirds. Dep. Agric. Stellenbosch S. Afr. Sci. Bull. 140:90.

Doehlert, D.C., M.S. McMullen, and N.R. Riveland. 2002. Sources of variation in kernel size in oats. Cereal Chem. 79:528–534.

Doehlert, D.C., and M.S. McMullen. 2001. Optimizing conditions for experimental oat dehulling. Cereal Chem. 78:675–679.

Doehlert, D.C., M.S. McMullen, and R.R. Baumann. 1999. Factors affecting groat percentage in oat. Crop Sci. 39:1858–1865.

Ganssmann, W. 1964. Vergleichende Untersuchungen der Qualitat von Industriehafer. Die Muhle und Mischfuttertechnik 101:776–779.

Ganssmann, W., and K. Vorwerck. 1995. Oat milling, processing and storage. p. 369–408. *In* R.W. Welch (ed.) The oat crop: Production and utilization. Chapman & Hall, London.

Hachmann, W. 1947. Hafermullerei: Grossensortierung vor dem Schalen. Getreide Mehl Brot 1:7–9.

Hubner, R. 1951. Vierjahrige Untersuchungen uber Kornqualitat und Leistungeschaften des Hafers. I. Morphologisch-physikalische Untersuchngen. Z. Acker Pflanzenbau 93:44–78.
Mader, W. 1927. Zur Frage der Bestimmung des 1000-Korngewichtes zur sortencharakteristik bei Hafer. Fortschr. Landw. 2:550–552.
Martin, C.R., R. Rousser, and D.L. Brabec. 1993. Development of a single kernel wheat characterization system. Trans. ASAE 36:1399–1404.
McLachlan, G., and D. Peel. 2000. Finite mixture models. John Wiley & Sons, New York
Milatz, R. 1933. Neue Hafersortenmerkmale. Angew. Bot. 15:481–518.
Otsu, N. 1979. A threshold selection method for gray level histogram. IEEE Trans. Syst. Man Cybern. SMC-9:62–66 IEEE, New York.
Pietrzak, L.N., and R.G. Fulcher. 1995. Polymorphism of oat shape in several Canadian oat cultivars. Can. J. Plant Sci. 75:105–109.
Peek, J.M., and L.M. Poehlman. 1949. Grain size and hull percentage as factors in the milling quality of oats. Agron. J. 41:462–466.
Salisbury, D.K., and W.R. Wichser. 1971. Oat milling-Systems and products. Bull. Assoc. Oper. Mill. 1971:3242–3247.
Steel, R.G.D., J.H. Torrie, and D.A. Dickey. 1997. Principles and procedures of statistics: A biometrical approach. 3rd ed. McGraw-Hill, Boston.
Sword, J. 1949. Milling values of oat varieties I. 1946 results. Scot. Agric. 28:137–148.
Symons, S.J., and R.G. Fulcher. 1988. Determination of variation in oat kernel morphology by digital image analysis. J. Cereal Sci. 7: 219–228.
Takeda, K., and K.J. Frey. 1980. Tertiary seed set in oat cultivars. Crop Sci. 20:771–774.
Zade, A. 1915. Methoden zur Bestimmung des Spelzenanteils beim Hafer. Fuhlings Landw. Z. 64:295–311.